

Online Research @ Cardiff

This is an Open Access document downloaded from ORCA, Cardiff University's institutional repository: <http://orca.cf.ac.uk/111574/>

This is the author's version of a work that was submitted to / accepted for publication.

Citation for final published version:

Li, Yu-Chao, Wei, Lulu, Cleall, Peter and Lan, JiWu 2018. Rankine theory-based approach for stability analysis of slurry trenches. *International Journal of Geomechanics* 18 (11) , 06018029. 10.1061/(ASCE)GM.1943-5622.0001288 file

Publishers page: [https://doi.org/10.1061/\(ASCE\)GM.1943-5622.0001288](https://doi.org/10.1061/(ASCE)GM.1943-5622.0001288) <[https://doi.org/10.1061/\(ASCE\)GM.1943-5622.0001288](https://doi.org/10.1061/(ASCE)GM.1943-5622.0001288)>

Please note:

Changes made as a result of publishing processes such as copy-editing, formatting and page numbers may not be reflected in this version. For the definitive version of this publication, please refer to the published source. You are advised to consult the publisher's version if you wish to cite this paper.

This version is being made available in accordance with publisher policies. See <http://orca.cf.ac.uk/policies.html> for usage policies. Copyright and moral rights for publications made available in ORCA are retained by the copyright holders.



31 **Introduction**

32

33 Slurry trenches are long narrow vertical excavations, typically used in the construction of
34 diaphragm walls in civil engineering or cut-off walls (vertical barriers) in
35 geoenvironmental engineering. During excavation, the trenches are filled with slurry,
36 which exerts pressure on the trench walls to balance the earth pressure and hydraulic
37 pressure from the surrounding soils, to prevent trench collapse (Li and Cleall 2017).

38

39 Stability of the slurry trench during excavation is a major concern in design and
40 construction. Coulomb-type force equilibrium methods considering a two-dimensional
41 wedge between the trench and a trial failure plane (Nash and Jones 1963; Morgenstern
42 and Amir-tahmasseeb 1965; Elson 1968; Filz et al. 2004) is typically used to analyze
43 slurry trench stability (Tsai and Chang 1996). The contribution of shear forces at the
44 sides of the planar wedge was taken into account by Piaskowski and Kowalewski (1965);
45 Prater (1973); Washbourne (1984); Tsai and Chang (1996) and Fox (2004). Such
46 Coulomb-type force equilibrium methods consider the whole failure mass as a wedge and
47 so cannot consider scenarios of trench excavation in heterogeneous layered soils since the
48 shear strength parameters on the trial slip surface are varied between the layers. The
49 horizontal slice method was applied in stability analysis of slurry trenches by Li et al.
50 (2013) for the scenario of layered soils; however, this method requires a computational
51 analysis to perform the force equilibrium analysis of the slices. In practice, variably
52 distributed surcharges from landfill berms, placed solid wastes, excavation machines or
53 nearby buildings may induce large deformation in the surrounding soils and even trench
54 collapses during excavation. For example, shallow trench failure and cracks in a nearby
55 landfill berm that occurred during and after trench excavation were observed at two sites
56 in China in 2017 (see Fig. 1). It is likely that the presence of additional surface
57 surcharges contributed to the failure and cracks.

58

59 In this paper, an approach for stability analysis of slurry trenches is proposed based on
60 Rankine's theory of active earth pressure. This approach is able to consider soil
61 stratification and varied distributed surcharges for slurry trench design. The proposed

62 approach is verified by analysis of a previously reported problem and is applied to a
63 scenario with a nearby slope.

64

65

66 **Theory**

67

68 A typical slurry trench in layered soils is illustrated in Fig. 2a. During trench excavation,
69 the trench is filled with slurry to avoid trench collapse. The pressure on the trench side
70 walls exerted by the slurry is typically less than the sum of the earth pressure at-rest and
71 hydrostatic pressure before excavation. So the trench side walls move inwards towards
72 the trench centerline (Filz 1996), which indicates the soils surrounding the trench tends
73 towards a state of active earth pressure from the at-rest state. During the process the
74 slurry in the trench penetrates into the surrounding soils and forms a low-permeability
75 “filter cake” on the trench side walls. In this paper, the forces on the filter cake from the
76 two sides (that is, the slurry side and the surrounding soil side) are considered (see Fig.
77 2b) and the factor of safety for the slurry trench, F_s , is defined by

$$78 \quad F_s = \frac{P_s - P_w}{P_a} \quad (1)$$

79 where P_s is the total thrust exerted by the slurry on to the filter cake; P_w is the total
80 hydrostatic force of the groundwater in the surrounding soils on to the filter cake; and P_a
81 is the total active thrust exerted on to the filter cake and is the sum of thrust by
82 surrounding soil and that by uniformly distributed surcharge. In Eq. (1), $P_s - P_w$, the
83 seepage force on solid particles of the filter cake, is the resistance to sliding. An
84 alternative definition of F_s , which is given in the following expression, was proposed by
85 Xanthakos (1994),

$$86 \quad F_s = \frac{P_s}{P_a + P_w} \quad (2)$$

87 A comparison between the two definitions of F_s is made in the next section.

88

89 For the problem considered, P_w and P_s can be written as follows,

90
$$P_s = \frac{1}{2} \gamma_s H_s^2 \quad (3)$$

91
$$P_w = \frac{1}{2} \gamma_w H_w^2 \quad (4)$$

92 where γ_s and γ_w are the unit weights of slurry and water, respectively; and H_s and H_w are
 93 the heights of the slurry surface and groundwater table, respectively, as illustrated in Fig.
 94 2a.

95
 96 P_a is calculated by Rankine's theory of earth pressure. The active earth pressure, which
 97 implies a lower bound plasticity solution, corresponds to the surrounding soils being at
 98 the state of plastic equilibrium, and can be written as follows,

99
$$p_{ai}^T = \sum_{k=1}^{k=i-1} \gamma_k h_k K_{ai} - 2c_i \sqrt{K_{ai}} + qK_{ai} \quad (5)$$

100
$$p_{ai}^B = \sum_{k=1}^{k=i} \gamma_k h_k K_{ai} - 2c_i \sqrt{K_{ai}} + qK_{ai} \quad (6)$$

101
$$K_{ai} = \tan^2(45^\circ - \phi_i / 2) \quad (7)$$

102 where p_{ai}^T and p_{ai}^B are the active earth pressures at the top and the bottom, respectively,
 103 of the i th soil layer; K_{ai} is the active earth pressure coefficient of the i th soil layer; q is a
 104 uniformly distributed surcharge; c_i and ϕ_i are the cohesion intercept and internal friction
 105 angle, respectively, of the i th soil layer; γ_k and h_k are the unit weight and thickness,
 106 respectively, of the k th soil layer. For the soil layers below the groundwater table the
 107 effective unit weight and the effective shear strength parameters are used. A soil layer
 108 intersected by the presence of the ground water table should be divided into two layers. It
 109 is noted that at the interface between soil layers the active earth pressure at the bottom of
 110 the upper soil layer may be not equal to that at the top of lower soil layer if the two soil
 111 layers have different properties parameters. Tension cracks are likely to develop near the
 112 surface and the part of the pressure distribution should be neglected if $qK_{a1} - 2c_1 \sqrt{K_{a1}} < 0$
 113 as illustrated in Fig. 2b. P_a can then be written as follows,

114
$$P_a = \sum_{i=1}^{i=n} \frac{(p_{ai}^T + p_{ai}^B) h_i}{2} \quad (8)$$

115 where n is the total number of the layered soils corresponding to the depth of the trench
 116 considered. For the scenario with layered soils, in contrast to the force equilibrium
 117 analysis of the horizontal slice method (Li, et al. 2013), P_a can be calculated by hand in
 118 the proposed method. It is noted that if the tension crack is filled with water the
 119 hydrostatic pressure must be considered (Barnes 2011).

120

121 As Rankine's theory is applied in this paper, the stress on the filter cake caused by varied
 122 distributed surcharges (Das 1998) can be taken into consideration in the stability analysis
 123 of slurry trenches. For the scenario where a slope is near the excavated slurry trench (see
 124 Fig. 3), the additional stress on the filter cake caused by the slope, Δp , can be calculated
 125 as follows (MOHURD 2012),

126

$$127 \quad \Delta p = \begin{cases} 0 & \text{for } z < a / \tan \theta \\ K_{ai} \frac{\gamma h}{b} (z - a) + K_{ai} \frac{E_a (a + b - z)}{b^2 K_a} & \text{for } a / \tan \theta \leq z \leq (a + b) / \tan \theta \\ K_{ai} \gamma h & \text{for } z \geq (a + b) / \tan \theta \end{cases} \quad (9)$$

$$128 \quad E_a = \frac{1}{2} \gamma h^2 K_a - 2ch\sqrt{K_a} + \frac{2c^2}{\gamma} \quad (10)$$

129 where z is the depth from the trench surface; a and b are the horizontal distance from the
 130 slope toe to the trench side wall and that of the slope face, respectively, as shown in Fig.
 131 3; θ is the spread angle and $\pi/4$ is recommended; h is the height of the slope; γ and c are
 132 the unit weight and cohesion intercept, respectively, of slope soil; E_a is the active earth
 133 pressure caused by the weight of the sloping part soil; and K_a is the active earth pressure
 134 coefficient of the slope soil using Eq. (7) with the cohesion intercept c and the internal
 135 friction angle ϕ of slope soil. The weighted average values of γ , c and K_a are used if the
 136 slope consists of varied layers.

137

138 For a typical case, the trench is in the most critical condition and has the minimum F_s
 139 when the trench is fully excavated to the designed depth. However, following the work
 140 of Li et al. (2013) it is recommended the values of F_s be calculated for the scenarios that

141 the trench is excavated to the bottoms of each soil layer, especially for layers with low
142 shear strength parameters in design.

143

144

145 **Verification and Investigation**

146

147 In this section, the proposed method is verified via analysis of a slurry trench stability
148 problem defined by Filz et al. (2004) and Fox (2006). The trench is 20 m deep and the
149 groundwater table is 3 m below the ground surface ($H_w=17$ m). The property parameters
150 for the soil layers above and below the groundwater table are: $\gamma_1=19$ kN/m³, $c_1=0$, $\phi_1=37^\circ$;
151 and $\gamma_2=20$ kN/m³, $c_2=0$, and $\phi_2=37^\circ$. The slurry surface is maintained at the ground
152 surface ($H_s=20$ m) and the unit weight of slurry is 11.8 kN/m³. No surcharge pressure is
153 applied on the ground surface ($q=0$). The unit weight of groundwater used in the
154 calculation is 10 kN/m³. The following calculations can be made using Eqs. (1), (3)~(8),

$$155 \quad P_s = \frac{1}{2} \times 11.8 \times 20^2 = 2360.0 \text{ kPa/m} \quad (11)$$

$$156 \quad P_w = \frac{1}{2} \times 10 \times 17^2 = 1445.0 \text{ kPa/m} \quad (12)$$

$$157 \quad K_{a1} = K_{a2} = \tan^2 \left(45^\circ - 37^\circ / 2 \right) = 0.249 \quad (13)$$

$$158 \quad p_{a1}^T = 0.0 \text{ kPa/m}^2 \quad (14)$$

$$159 \quad p_{a1}^B = p_{a2}^T = (19 \times 3) \times 0.249 = 14.2 \text{ kPa/m}^2 \quad (15)$$

$$160 \quad p_{a2}^B = (19 \times 3 + 10 \times 17) \times 0.249 = 56.5 \text{ kPa/m}^2 \quad (16)$$

$$161 \quad P_a = \frac{(0.0 + 14.2) \times 3}{2} + \frac{(14.2 + 56.5) \times 17}{2} = 622.2 \text{ kPa/m} \quad (17)$$

$$162 \quad F_s = \frac{2360.0 - 1445.0}{622.2} = 1.47 \quad (18)$$

163

164 As shown above, hand calculation can be performed for the stability analysis of slurry
165 trenches when the proposed approach is used. The F_s obtained by the proposed method is
166 1.47, which is the same as reported by Filz et al. (2004) and Fox (2006) using Coulomb

167 force equilibrium methods. Additional calculations on other published examples, that is,
 168 the example with full tension cracks of Fox (2004) and the example with $\beta=0^\circ$ of Li et al.
 169 (2013), were also performed and the results confirm that the proposed approach gives
 170 identical values of F_s to those obtained by Coulomb force equilibrium methods. The
 171 sliding resistance term, $P_s - P_w$, is implicitly considered in the equations of the Coulomb
 172 force equilibrium methods (see Eq. (2a) in Filz, et al. (2004) and Appendix) and is
 173 regarded as the sliding resistance in the proposed definition of F_s (see Eq. (1)) The same
 174 expression in terms of P_s and P_w used in these two methods results in an identical value
 175 of F_s . However, the definition of F_s presented by Xanthakos (1994) in Eq. (2) gives

$$176 \quad F_s = \frac{2360.0}{622.2 + 1445.0} = 1.14 \quad (19)$$

177 which is much lower than that reported by Filz et al. (2004) and Fox (2006). In this
 178 definition, the filter cake is in effect regarded as a fully impermeable layer, which causes
 179 a hydraulic discontinuity between the two sides of the filter cake. This definition is
 180 similar to the factor of safety against sliding of gravity retaining walls with the sliding
 181 resistance between the wall base and the soil beneath replaced by the thrust exerted by the
 182 slurry on to the filter cake.

183

184 Based on the problem above, the scenario with a nearby slope is considered. The
 185 horizontal distance from the slope toe to the trench side wall is 2 m ($a=2$ m). The
 186 inclination of the slope is 45° (that is, $b=h$). The cohesion intercept and internal friction
 187 angle of the slope soil are 5 kPa and 30° , respectively ($c=5$ kPa and $\phi=30^\circ$). The unit
 188 weight of slope soil is 18 kN/m^3 ($\gamma=18 \text{ kN/m}^3$). The additional stress on the filter cake
 189 caused by the slope with a height from 0.0 m to 5.0 m is calculated with $\theta=\pi/4$ used. For
 190 example, when $h=2.0$ m,

$$191 \quad \Delta p = \begin{cases} 0 \text{ kPa} & \text{for } z < 2\text{m} \\ 3.88z - 6.55 \text{ kPa} & \text{for } 2\text{m} \leq z \leq 4\text{m} \\ 8.96 \text{ kPa} & \text{for } z \geq 4\text{m} \end{cases} \quad (20)$$

192 The total additional force on the filter cake exerted by the slope, ΔP , is

$$193 \quad \Delta P = \frac{1.21 + 8.96}{2} \times 2 + 8.96 \times 16 = 153.5 \text{ kPa} \quad (21)$$

194 With a consideration of the additional force exerted by the slope, the factor of safety of
195 the slurry trench defined by Eq. (1) is

$$196 \quad F_s = \frac{2360.0 - 1445.0}{622.2 + 153.5} = 1.18 \quad (22)$$

197 Fig. 4 shows the relationship between the factor of safety (F_s) and the height of slope (h)
198 for $h=0.0$ m to 5.0 m. The value of F_s defined by Eq. (1) is reduced from 1.47 to 1.1,
199 which is typically the criterion for geotechnical structures in short-term condition, as h
200 increases from 0.0 m to 2.75 m and becomes less than 1.0 when $h>4.0$ m. From the
201 calculation of the scenarios considered, it can be seen that the stability of slurry trench is
202 sensitive to the surcharge from a nearby slope. Neglect of the additional stress from the
203 nearby slope results in non-conservative F_s in stability analysis of slurry trenches. Fig. 4
204 also gives the relationship between F_s defined by Eq. (2) and h . The value of F_s is less
205 than that defined by Eq. (1), which indicates it is relatively conservative, when $F_s>1.0$;
206 however, it turns to be greater than that defined by Eq. (1) when $F_s<1.0$; the values of F_s
207 defined by Eqs. (1) and (2) are equal when $F_s=1.0$, which corresponds to $P_s=P_a+P_w$.

208

209 **Conclusions**

210

211 This paper presents an approach for stability analysis of slurry trenches based on the
212 Rankine's theory of active earth pressure. The scenarios with soil stratification and
213 varied distributed surcharges can be analyzed via hand calculation when the presented
214 approach is used. The verification example shows the proposed definition of the factor of
215 safety gives identical value of F_s with the Coulomb force equilibrium methods. Further
216 investigation indicates the stability of slurry trench is sensitive to the surcharge from a
217 nearby slope, which requires attention in design. It is noted that in the presented
218 approach a two-dimensional analysis is performed and so the side force on the sliding
219 mass is not included, and so yielding a conservative result.

220

221

222 **Acknowledgement**

223

224 The financial supports received from the National Natural Science Foundation of China
 225 (NSFC) by grant No. 41672284 and the Science Technology Department of Zhejiang
 226 Province by grant No. 2015C03021 and 2016C31G2010015 are gratefully acknowledged.

227

228

229 **Appendix**

230

231 The Coulomb's force equilibrium method is recast herein to demonstrate the term $P_s - P_w$
 232 in the calculation of the factor of safety for slurry trenches.

233

234 As illustrated in Fig. 5, the limit equilibrium of the failure wedge is considered. The
 235 angle of the trial failure plane from the horizontal is α . The force on the hydrostatic
 236 pressure on the trial failure plane U can be decomposed into U_x and U_y , which are
 237 respectively,

$$238 \quad U_x = \frac{1}{2} \gamma_w H_w \frac{H_w}{\sin \alpha} \sin \alpha = \frac{1}{2} \gamma_w H_w^2 = P_w \quad (23)$$

$$239 \quad U_y = \frac{1}{2} \gamma_w H_w \frac{H_w}{\sin \alpha} \cos \alpha = \frac{1}{2} \gamma_w H_w^2 \cot \alpha \quad (24)$$

240 It is noted that $U_x = P_w$ in Eq. (23). Summing force components for the failure wedge in
 241 the horizontal and vertical directions,

$$242 \quad P_s + S \cos \alpha = U_x + N' \sin \alpha \quad (25)$$

$$243 \quad W = U_y + N' \cos \alpha + S \sin \alpha \quad (26)$$

244 where S is the shear force on the failure plane; N' is the effective normal force on the
 245 failure plane and W is the weight of the failure wedge. It can be observed that U_y is equal
 246 to the buoyant force on the failure wedge, so we define W' as follows,

$$247 \quad W' = W - U_y \quad (27)$$

248 where W' is calculated with the buoyant weight used for the portion of the failure wedge
 249 below the groundwater table. The shear force on the failure plane S is calculated as

$$250 \quad S = \frac{C + N' \tan \phi'}{F_s} \quad (28)$$

251 where C is the total cohesion force on the failure plane.

252 The following equation can be obtained using Eqs. (23), (25)~(28),

$$253 \quad \frac{\cos \alpha + \frac{\tan \phi'}{F_s} \sin \alpha}{\sin \alpha - \frac{\tan \phi'}{F_s} \cos \alpha} (P_s - P_w) + \left(\frac{\cos \alpha + \frac{\tan \phi'}{F_s} \sin \alpha}{\sin \alpha - \frac{\tan \phi'}{F_s} \cos \alpha} \frac{\cos \alpha}{F_s} + \frac{\sin \alpha}{F_s} \right) C - W' = 0 \quad (29)$$

254 The factor of safety F_s is implicitly included in Eq. (29) and can be calculated using
255 mathematic or numerical methods. The minimum F_s should be found by searching for
256 the critical inclination angle of α . It can be observed that P_s and P_w in Eq. (29) are only
257 shown by the term $P_s - P_w$. It is noted that the search of the critical inclination angle of
258 failure wedge is not required in the proposed approach.

259

260

261 **References**

262 Barnes, G. E. (2011). *Soil Mechanics: Principles and Practice*, Palgrave MacMillan.

263 Das, B. M. (1998). *Principles of Foundation Engineering*, Brooks/Cole Publishing
264 Company, Pacific Grove, California, USA.

265 Elson, W. K. (1968). "An experimental investigation of the stability of slurry
266 trenches." *Geotechnique*, 18, 37-49.

267 Filz, G. M. (1996). "Consolidation stresses in soil-bentonite backfilled trenches."
268 *The 2nd International Congress on Environmental Geotechnics*, K. Kamon, ed., Balkema,
269 Rotterdam, Osaka, Japan, 497-502.

270 Filz, G. M., Adams, T., and Davidson, R. R. (2004). "Stability of long trenches in
271 sand supported by bentonite-water slurry." *Journal of Geotechnical and*
272 *Geoenvironmental Engineering, ASCE*, 130(9), 915-921.

273 Fox, P. J. (2004). "Analytical solutions for stability of slurry trench." *Journal of*
274 *Geotechnical and Geoenvironmental Engineering, ASCE*, 130(7), 749-758.

275 Fox, P. J. (2006). "Discussion of "Stability of long trenches in sand supported by
276 bentonite-water slurry" by George M. Filz, Tiffany Adams, and Richard R. Davidson."
277 *Journal of Geotechnical and Geoenvironmental Engineering, ASCE*, 132(5), 666-666.

278 Li, Y.-C., and Cleall, P. J. (2017). "Slurry trench." *Encyclopedia of Engineering*
279 *Geology*, P. Bobrowsky, and B. Marker, eds., Springer.

280 Li, Y. C., Pan, Q., and Chen, Y. M. (2013). "Stability of slurry trenches with
281 inclined ground surface." *Journal of Geotechnical and Geoenvironmental Engineering*,
282 139(9), 1617-1619.

283 Li, Y. C., Pan, Q., Cleall, P. J., Chen, Y. M., and Ke, H. (2013). "Stability Analysis
284 of Slurry Trenches in Similar Layered Soils." *Journal of Geotechnical and*
285 *Geoenvironmental Engineering*, 139(12), 2104-2109.

286 MOHURD (Ministry of Housing and Urban-Rural Development of the People's
287 Republic of China). (2012). "Technical specification for retaining and protection of
288 building foundation excavations, JGJ 120-2012." China Architecture & Building Press,
289 Beijing.

290 Morgenstern, N., and Amir-tahmassebi, I. (1965). "The stability of a slurry trench in
291 cohesionless soils." *Geotechnique*, 15(4), 387-395.

292 Nash, J. K. T. L., and Jones, G. K. (1963). "The support of trenches using fluid
293 mud." *Proceedings of Grouts and Drilling Muds in Engineering Practice* Butterworths,
294 London, 177-180.

295 Tsai, J. S., and Chang, J. C. (1996). "Three-dimensional stability analysis for slurry-
296 filled trench wall in cohesionless soil." *Canadian Geotechnical Journal*, 33(5), 798-808.

297 Xanthakos, P. P. (1994). *Slurry walls as structural systems*, McGraw Hill, New
298 York.

299

300 **List of Figure Captions**
301

302 Fig. 1 Cases of shallow trench failure and large deformation in nearby landfill berm
303 induced by slurry trench excavation: (a) Case 1, Shallow trench failure; (b) Case 2,
304 Cracks in nearby landfill berm.

305 Fig. 2 Configuration of a slurry trench and pressures on 'filter cake'.

306 Fig. 3 Lateral earth pressure caused by a nearby slope on the surface.

307 Fig. 4 Relationship between the factor of safety and the height of nearby slope.

308 Fig. 5 Configuration of a slurry trench for Coulomb's force equilibrium method.

309



316
 317
 318
 319
 320



Longitudinal crack on landfill berm surface



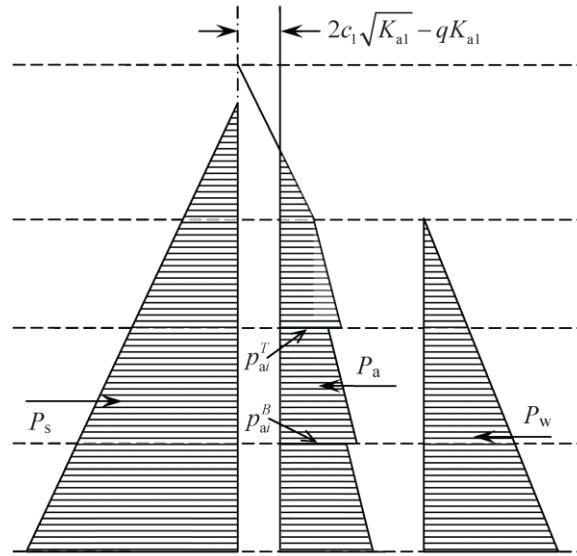
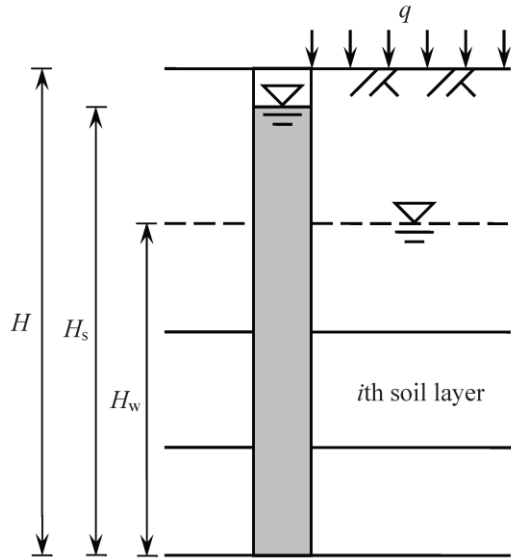
Slurry trench

Landfill berm



Transverse cracks on landfill berm surface at turning cover

321



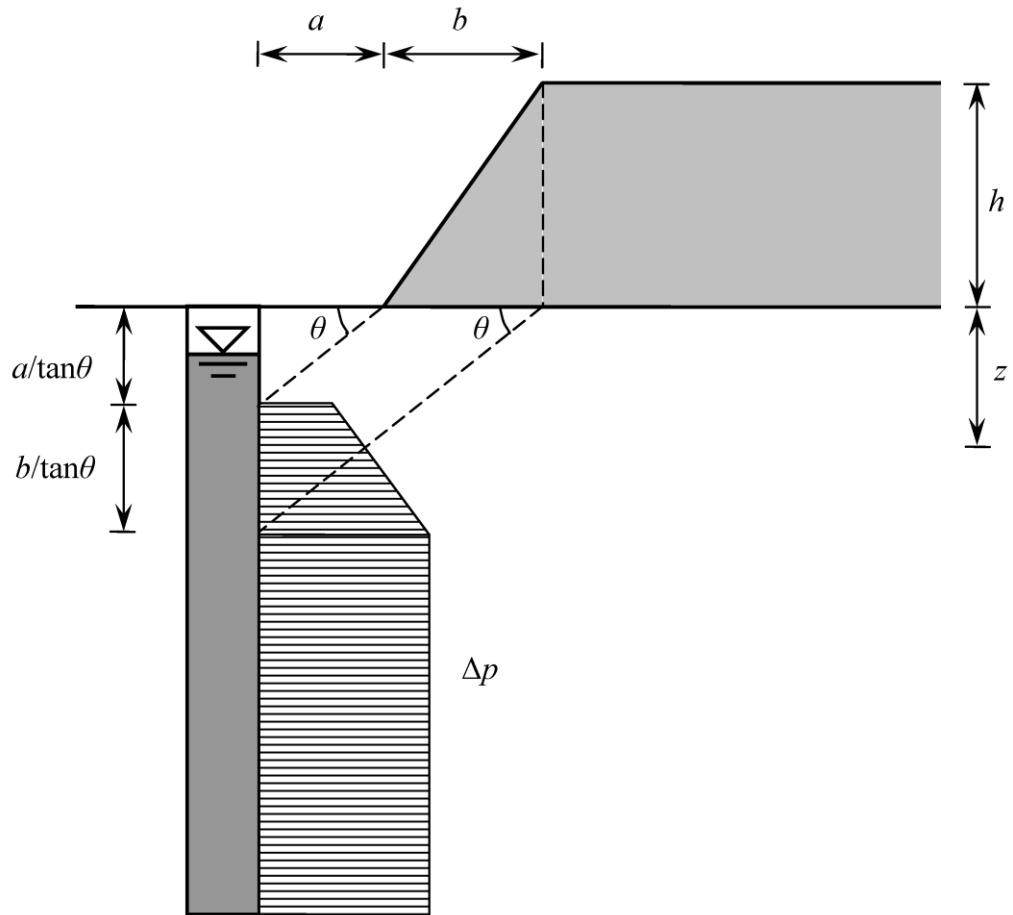
322

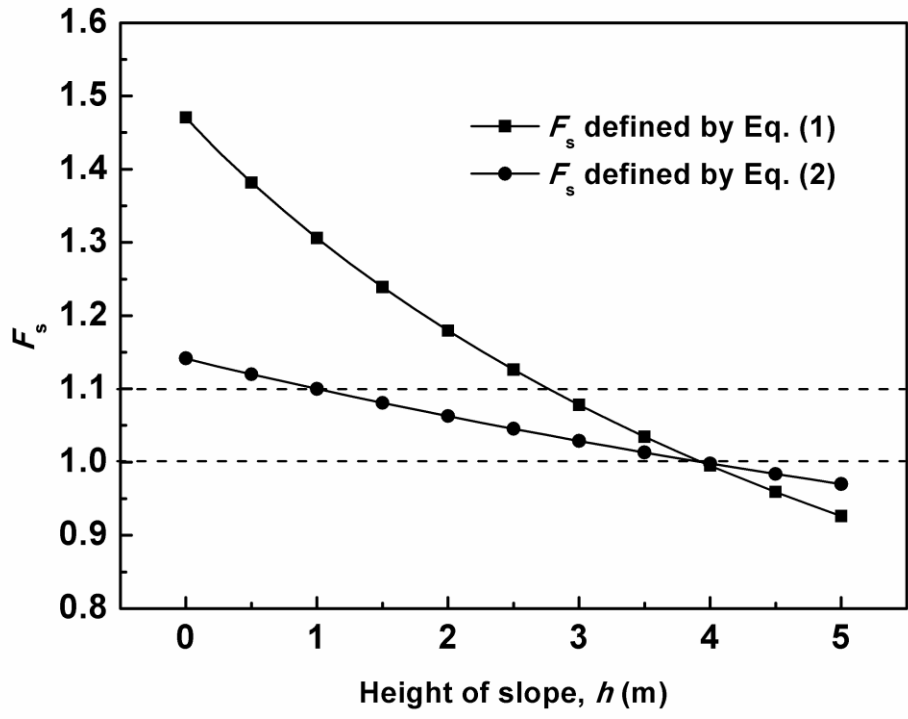
323

324

325

326





327

328

